energies

MDPI

Article

Impact of Energy Losses Due to Failures on Photovoltaic Plant Energy Balance

Isidoro Lillo-Bravo [1,*], Pablo González-Martínez [1], Miguel Larrañeta [2] and José Guasumba-Codena [3]

[1] Department of Energy Engineering, Universidad de Sevilla, Camino de los Descubrimientos s/n, 41092 Seville, Spain; pabgonmar1@gmail.com
[2] Andalusian Association for Research and Industrial Cooperation (AICIA), Camino de los Descubrimientos s/n, 41092 Sevilla, Spain; mlarraneta@gter.es
[3] Renewable Energy Laboratory, Universidad de las Fuerzas Armadas, 171103 Sangolquí, Ecuador; sjguasumba@espe.edu.ec
* Correspondence: isidorolillo@us.es; Tel.: +34-954-487-236

Received: 13 December 2017; Accepted: 29 January 2018; Published: 3 February 2018

Abstract: Photovoltaic (PV) plant failures have a significant influence on PV plant security, reliability, and energy balance. Energy losses produced by a PV plant are due to two large causes: failures and inefficiencies. Knowing the relative influence of energy losses due to failures and energy losses due to inefficiencies on the PV plant energy balance contribute to the optimization of its design, commissioning, and maintenance tasks. This paper estimates the failure rates, grouped by components, and the relative impact of the failures on the PV plant energy balance through real operation and maintenance follow-up data of 15 PV plants in Spain and Italy for 15 months. Results show that the influence of failures in energy losses of all analysed PV plants is low, reaching a maximum value of 0.96% of the net energy yield. Solar field energy losses only represent 4.26% of all failure energy losses. On the other hand, energy losses due to inefficiencies have represented between 22.34% and 27.58% of the net energy yield.

Keywords: photovoltaic (PV); energy losses; failures

1. Introduction

As the photovoltaic market is growing rapidly based on improvements in photovoltaic (PV) modules, manufacturing advances, economies of scale and cost reduction [1], reliability, failures, and their associated energy losses, more questions are beginning to be asked.

According to the project report, Technical Risks in PV Projects [2], failures can be categorised into components (modules, inverters, mounting structure, connection and distribution boxes, cabling, potential equalization and grounding, lightning and protection system, weather station, communication and monitoring, transformer station, infrastructure and environmental influence, storage system, and miscellaneous) and phases (product testing, photovoltaic (PV) plant planning/development, installation/transportation, operation/maintenance, and decommissioning) of the value chain of a PV project.

During the operation/maintenance phase, failures can be found in the PV array such as snail trail [3], hot spot, diode failure, EVA discoloration, glass breakage, delamination with breaks in the ribbons and solder bonds [4], light induced degradation [5], low irradiance losses [6], potential induced degradation [7], shading effect [8], soiling effect [9], sun tracking system misalignments [10], wiring losses [11], mismatching effect in solar array [12], and other failures such as ground faults, line-to-line faults, and arc faults; although there have not been many such failures, a recent fire suggests the need for improvements to avoid them [13].

The failures types of PV modules are highly dependent on the design and technology of the PV module and on the environmental conditions in which the module is deployed. Hasselbrink et al. summarized data for returns from a fleet of more than 3 million modules, from 20 manufacturers [14]. The study found that 0.44% of the modules were returned after an average deployment of 5 years, with the vast majority of the returns associated with failures that can usually be identified visually, though there could be bias in this data, since modules with no visual defects would be harder to identify by the customer. A 2017 report from the National Renewable Energy Laboratory [15] examined 54,500 PV systems installed between 2005 and 2015. They found a median failure rate of just 5 out of 10,000 modules annually, which comes out to a 0.05% failure rate in all photovoltaic modules. In general, reported degradation percentages appear to have decreased appreciably in newer installations that were deployed after the year 2000. The report highlighted that modules in hot and humid climates show considerably higher degradation modes than those in desert and moderate climates, which warrants further investigation. Delamination and diode/j-box issues are also more frequent in hot and humid climates than in other climates. The highest concerns of systems installed in the last 10 years appear to be hot spots followed by internal circuitry discoloration. Encapsulant discoloration was the most common degradation mode, particularly in older systems. In newer systems, encapsulant discoloration appears in hotter climates, but to a lesser degree. Thin-film degradation modes are dominated by glass breakage and absorber corrosion, although the breadth of information for thin-film modules is much smaller than for x-Si.

In addition to failures, there are also other technical risks during operation phase due to degradation. For instance, Jordan et al. reviewed potential degradation rates of PV modules and systems reported in published literature from field testing throughout the last 40 years. Nearly 2000 potential degradation rates, measured on individual modules or entire systems, have been assembled from the literature, showing a median value of 0.5%/year [16].

Apart from PV modules, PV plants use inverters in a wide array of sizes and topologies, which complicates the evaluation of inverter failure rates. The majority of inverter failure studies do not treat the inverter as one black box. The reliability of PV inverter depends on the performance of each component. Inverters have failures such as failure in the insulated-gate bipolar transistor [17], surge protection, maximum power point tracker failure [18], alternating current (AC) or direct current (DC) contactors, electrolytic capacitors [19] fuses, control software, monitoring system, and inefficiency due to overheating. In particular, in grid-connected PV systems, a PV inverter may handle a high level of power flow and operate in a high temperature environment, which degrades the inverter reliability and increases the risk of component aging failures. According to Flicker et al., the failure modes that mostly affect PV inverters are related to units exposed to high thermal and electrical stress, as well as to the thermal management system itself [20]. Chang et al. investigated different circuit topologies of the single-phase PV inverters [21]. Results indicate that failures often occur in the switching stage, and temperature is the most likely cause of failure. Peng Zhang et al. analysed the reliability of the three main components: power electronic switches with a failure rate dominated by thermal overstress; capacitors with a failure rate that is dependent on the applied DC voltage, ripple current, and ambient conditions (temperature, airflow, and heat sinking); and inverter topologies in which results show that higher system reliability can be achieved by using module-integrated inverters [22].

Besides, PV plants are connected to an electrical grid that can present failures such as shutdown and overvoltage [23]. Moreover, many PV plants include transformer stations that also can presents failures such as electrical protection setting failure and overheating [24].

There are others failures in PV plants such as weather stations failures (pyranometer, calibrated reference cells, temperature sensors failures), fixed structure (rust on bolt and structure), ground (drainage and tracks damage), perimeter fence damages, and security system and monitoring system failures, but they do not directly affect energy losses and the electrical grid.

Extracting accurate trends of failure rates and their impact is difficult. There is a wide variety of equipment with unknown manufacturing and installation quality, PV array and inverter configurations, PV modules tracker systems, equipment technology, climate, electrical grid quality, equipment operation time, inspection methodologies, how the inspection sheet has been reported, and even what is the definition of the failure rate. Despite this, the overarching failure rates are usually used by reliability analysis methods, such as the Markov method [25], Fault Tree Analysis [26], Monte Carlo simulation [27], Pareto analysis [28], and the state enumeration method [29].

Moreover, it is even more difficult to know the true influence of failure on the PV plant energy balance, because there are many circumstances that affect them. For instance, one failure in a PV module could affect the energy yield of other PV modules and even could affect the inverter efficiency. Consequently, both failures and the energy losses associated with them are significant and must be clear in order to improve of PV market. Energy losses due to failure are an essential form of data that can be used to calculate associated costs.

With regard to energy balance, the performance ratio (PR) is the main rate used to know the impact of all energy losses on the PV plant energy balance without taking into account the PV module efficiency. It is the ratio of utilizable AC electricity at the feed-in meter to the amount of energy, which could be generated in case modules that were operated under Standard Test Conditions (STC), (1000 W/m^2, 25 °C, AM 1.5) continuously and without any further losses in the system. It is defined in the standard IEC 61724-1:2017. PR could reach a value of more than 0.8 for recent PV plants [30]. Nevertheless, with the PR it is impossible to know clearly the energy losses related to failure with respect to the energy losses related to inefficiencies in the PV plant. If the PV plant would include batteries, the energy balance could also be affected by the control strategies for energy store [31].

In addition to failures, inefficiencies of the PV plant components and their influence on the energy losses have been studied individually. For instance, in the PV array, the influence of a non-uniform of solar radiation on the module plane has always been one of the major concern for PV plants, so the effects of shading, snowing, and soiling on the output power have been extensively studied [9,32,33]. Another significant effect is the temperature influence according to PV technology. For instance, for the temperature, effect negative temperature coefficients are found for the crystalline module. On the contrary, for the amorphous module, positive power temperature coefficients can even be found, due to light soaking and thermal annealing effects. This shows that the data sheet temperature parameters do not reflect the annual thermal response of the module, and no reliable results using such coefficients could be achieved [34]. Another difference is the seasonal performance behaviour among PV technologies. PV technologies have a different response to temperature and the level of irradiance and its characteristics, mainly the angle of incidence and spectral effects. All of these effects should be taken into account to estimate their performance [35]. Amorphous thin film technology seems more suitable for building-integrated photovoltaic plants in cloudy or hot sites, while crystalline technology is suitable for open rack installation in sunny and cold locations [36].

In the inverter, the effect of the inverter temperature and maximum power point tracking are another significant concern of inefficiency. The temperature effect on the inverter efficiency, output power, and failure probability has also been analysed [37], and several maximum power point tracking methodologies have been proposed [38].

However, the influence of all PV plant failures and their relative impact on the whole PV plant energy balance has not been sufficiently researched. Gabriele et al. realize a study of reliability for PV plants between 2.5 kWp and 100 kWp up to the entry of the transformer station. To achieve more reliability, they conclude with the necessity of a high preventive maintenance and monitoring of the PV field (module and string protections) and a normal preventive maintenance of inverters. We propose only monitoring for the rest of components of the PV plant (AC circuit breaker, grid protection, DC Switch, AC Switch, differential circuit breaker and connector) [39]. Anastasios makes a thorough analysis of the failures of a great number of PV arrays and inverters, at two levels: one level is named the failure area that contains information about the item which exhibited an issue; and the second level is named the root cause that tracks the reason behind the issue. He highlights that the limited capability for deep failure analysis may dampen the value of the collected information [40]. In the same vein, Hasselbrink et al. indicate that collecting the failure data in a systematic format greatly simplifies the subsequent analysis [14].

To analyse the economic consequences of these risks, the Solar Bankability project [2] implemented a cost-based failure modes and effects analysis to the PV sector and defined a methodology for the estimation of economic losses due to planning failures, system downtime, the substitution/repair of components, and the assessment of the effectiveness of mitigation measures. The methodology is based on statistical analysis. The quality of the analysis depends on the amount of failure data available and on the assumptions taken for the calculation of a Cost Priority Number (CPN). This methodology is being enhanced by other authors [41] and paves the way to a desirable standardisation.

No studies that include the relative influence of energy losses due to failures on the global energy balance of the PV plant based in real data have been found. Only a comparison of the energy losses related to a single PV module failure for a base and worst-case scenario has been found [2]. In this case, it is not considered that in a PV array, the energy losses due to a PV module failure are strongly influenced by the energy yield of other modules without failure connected in series or parallel to it. Most PV plant simulation software estimates that PV plant energy losses are associated with inefficiencies but not due to failures [42,43]. In many cases, there is a significant difference between predicted and measured energy yield [44].

The current study, which focuses on the operation phase of a PV system, contributes to the analysis of the relative impact of energy losses due to failures in the PV plant energy balance, in 15 PV plants, located in Spain and Northern of Italy, with different PV module technologies, mounting configurations, and power. All of these PV plants have been in operation since 2010–2011. The knowledge of the relative impact of energy losses due to failures on the PV plant energy balance is useful to better estimate the energy losses cost and to improve maintenance and mitigation measures.

2. Methodology to Assess Energy Losses Due to Failure

The maximum electrical output energy of a photovoltaic array (*ME*) really is impossible to achieve in a PV plant performance, because it is affected by energy losses produced by failure energy losses (*FEL*) and energy losses produced by performance energy inefficiencies (*PEL*). The IEC 60050-191 defines failure as "the termination of the ability of an item to perform a required function" [45]. In this study failure is considered the total or partial malfunction of one or more equipment of the PV plant being unavailable for production.

According to the above definition, failures necessarily require corrective maintenance. Within the group of failures that affect *FEL* has been included PV module failure, which has led to it being replaced according to the warranty or performance conditions, such as glass broken, major delamination and hot spots, internal circuitry failure, solder bond failure and diode failure, inverter failure, or transformer failure such as shutdown or disconnection from the electrical grid.

PEL are the sum of the following energy losses. The energy losses produced by evitable inefficiencies are due to a not optimal performance of one or more equipment of the PV plant; in these cases, the equipment operates but at a level below expectations. In many cases, inefficient performance does not require immediate corrective action. There are multiple causes of these types of energy losses such as module temperature effect, bubbles, discoloration, chalking, potential induced degradation, shading and soiling effect, PV modules degradation, sun tracking system misalignments, wiring losses, mismatching effect in solar array, and inverter overheating. In some of these cases, such as mismatching effect, maximum power point tracker losses, PV module degradation, wiring losses, and shading phenomena are difficult to avoid when the PV plant is finished and in operation. Other failures such as derating effect, soiling effect, and sun tracking system misalignment may be corrected. Failures associated with these evitable inefficiencies usually take longer to manifest and require more sophisticated analytics to identify the corrective action than failures associated with *FEL* [40].

The energy losses produced by inevitable inefficiencies are due to the expected performance of one type of equipment, according to the nominal operation conditions described by the manufacturer.

For instance, an inverter always has energy losses produced during its performance reflected by the manufacturer by its efficiency curve with the conditions set. These energy losses are inevitable for a given equipment and performance conditions. Global energy losses due to inefficiencies *PEL* are the sum of both inevitable and evitable inefficiencies.

So, based on these definitions, a PV plant in real operating conditions produces an electrical energy output at the feed-in meter, (*RE*), significantly lower than *ME*, related to both types of losses, with *FEL* and *PEL* using the energy balance shown in Equation (1).

$$ME = RE + PEL + FEL \tag{1}$$

FEL of a PV plant can be calculated according to equations shown in Appendix A, and *ME* can be calculated according to Equation (2) [46].

$$ME = P_n \cdot \sum_{t=1}^{t=h} \frac{GTI_t}{1000} \cdot (1 - \gamma \cdot \Delta T_{cell\_t}) \tag{2}$$

in which

- P_n (kWp) is the peak power of the PV plant in Standard Test Conditions (STC).
- γ (%/K) temperature coefficient for power (negative in sign) that corresponds to the installed modules.
- ΔT_{cell_t} (K) is the difference between the average hourly temperature of the PV reference module of the PV plant at hour t and 298.15 K.
- h is the hour number of the analysed period.
- GTI_t (W/m^2) is the global tilted irradiance in the hour t on the module plane.

Energy losses due to inefficiencies of a generic PV plant, *PEL* could be calculated as:

$$PEL = ME - RE - FEL \tag{3}$$

FEL and *PEL* are related to the PV plant hourly correct performance ratio PR_{corr} according to Equation (4).

$$PEL + FEL = RE \cdot (1 - PR_{corr}) / PR_{corr} \tag{4}$$

in which PR_{corr} is the hourly corrected performance ratio, determined according to Equation (5) [46]. Highlight that with this definition of PR_{corr}; *PEL* does not include the energy loss due to the PV module performances at module temperature instead of at module temperature in STC (29,815 K).

$$PR_{corr} = RE / (P_n \cdot \sum_{t=1}^{t=h} \frac{GTI_t}{1000} \cdot (1 - \gamma \cdot \Delta T_{cell\_t}) \tag{5}$$

Using these equations, it is possible to estimate the relative influence of *FEL* and *PEL* separately on *ME* and *RE* by assuming in this paper the following hypotheses:

- In the calculation of energy losses caused by a failure, the failure time considered includes the lapse of time between the hour in which the failures has been detected, (t_d), until the hour in which the failure has been repaired (t_r). We do not consider the lapse of time between the real occurrence of the failure until it is detected because it is not known.
- The performance ratio during the failure time is considered the average performance ratio of the PV plant in the 15 months defined by Equation (5). In this equation, we have utilized the hourly measured data of energy production, solar radiation on the plane of the modules measured by a pyranometer, and module temperature.
- In the quantification of the energy losses associated with a failure, we take into account the equipment that failed and the remaining equipment that is affected upstream of the one that

failed, taking into account the global hourly radiation on the level of the PV array, the average hourly temperature of the panel during the dwell time, the average performance ratio of the PV plant during the 15 months, and the dwell time, from the t_d hour in which the failure is detected until the t_r hour that the failure has been repaired.

- When a failure takes place in a PV module its associated energy losses have been calculated assuming that in the time period between when the failure is detected and is replaced, the module there has not produced electric power in the complete string that the PV module belongs.
- Energy losses due to the transformation of solar radiation into electricity by a PV module in STC according to its datasheet have not been considered in *PEL* estimation.
- The PV plant energy losses due to a failure produced in the period from the moment when the failure took place and the instant in which it has been detected have been included in *PEL* estimation.

To estimate the influence of equipment failure and technology involved in the energy losses, the following criteria has been defined:

Criterion 1: Failures have been grouped depending on the affected equipment. Total failures, (TF), have been broken down into failures in the solar field, (TF_{SF}), inverter, (TF_I), transformer station, (TF_{ST}), electrical grid, (TF_G), and monitoring system, (TF_{MS}), according to Figure 1.

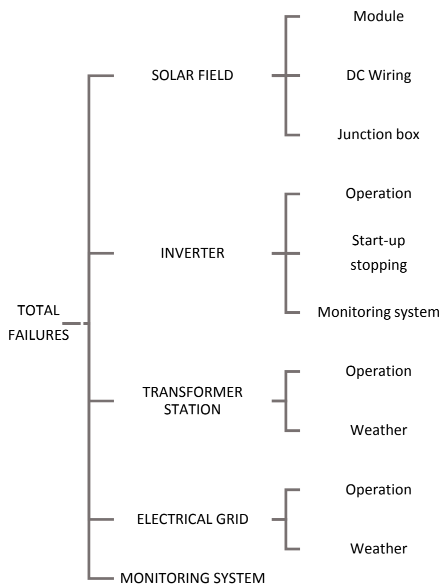

Figure 1. Classification of failures according to the affected equipment.

Within the solar field, failures have been broken down into failures that have led to the replacement of the photovoltaic module, failures in the DC wiring, and failures in the junction box, included fault in protections (not right performance of protection for fault in other equipment).

The inverter failures have been broken down into operation failures, failures of start-up and stopping, and failures in its monitoring system. Within the transformer station, failures have been broken down into failures in the transformer protections due to operation causes (not right performance of protection for fault in other part of the equipment) and failures resulting from extreme weather situations. Within the electrical grid, failures have been broken down into operation inherent grid failures and failures resulting from extreme weather situations.

Failures are not broken down into a more detailed root cause classification, because although the issue is logged in the database the true root cause was unknown, or it was inappropriately described or annotated in a wrong way by the professional supervision service in some cases. For this reason, we have limited the aim of the article according to the quality of the data set [36]. For instance, an inverter shutdown may be caused by different issues: insulated-gate bipolar transistor, surge protection, overheating, AC or DC contactors, electrolytic capacitors, fuses, control software, and power supply. Sometimes, the true root cause was not professionally described. For this reason, according to the aim of this article, all of them have been grouped into operation failures associated with the inverter.

Criterion 2: This classification is based on the technology linked to the failure, distributed in photovoltaic, electrical, electronic, and telecommunication technologies according to the Figure 2.

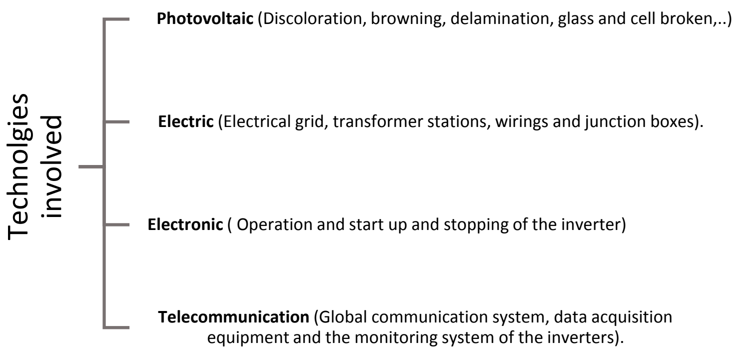

Figure 2. Classification of failures according to the involved technology.

Failures occurred in the PV module such as discoloration, browning, delamination, glass, and cell breakage corresponding to replacement of the photovoltaic module have been assigned to PV technology failures.

In the group of electrical technology, failures have been included: failures related to electrical grid, transformer stations, wirings, and junction boxes.

In the group of electronic technology, failures have been included in the operation, start up, and stopping of the inverter failures. In the group of telecommunication technology, failures have included failures in the global communication system, the data acquisition equipment, and the monitoring system of the inverter.

Failure rates calculated for each PV plant have been defined as:

Annual failure rate in the solar field of the PV plant per module of the PV plant, *FRSF* (failures/year·module):

$$FRSF = TF_{SF} \cdot 12/(15\ Module\ number) \quad (6)$$

Annual failure rate in the inverter of the PV plant per inverter in the PV plant, FRI_{in}. (failures/year·inverter):

$$FRI = TF_{I} \cdot 12/(15 \cdot Inverter\ number) \quad (7)$$

Annual failure rate in the station transformation of the PV plant, *FRST*, (failures/year):

$$FRST = TF_{ST} \cdot 12/15 \quad (8)$$

Annual failure rate in the electrical grid of the PV plant, *FRG*, (failures/year):

$$FRG = TF_{G} \cdot 12/15 \quad (9)$$

Annual failure rate in the monitoring system of the PV plant, *FRM*, (failures/year):

$$FRM = TF_{M} \cdot 12/15 \quad (10)$$

Annual total failures rate of the PV plant, *TFR*, (failures/year):

$$TFR = TF \cdot 12/15 \quad (11)$$

3. Application and Results

The methodology has been applied to 153 PV installations of 15 PV plants located in Spain and Northern Italy as shown in Figure 3 in a 15-months period, from January 2014 to March 2015. All these plants were put into operation in the period of 2010–2011 so they had already been more than three years of operation and adjustments of their set-up. All analysed PV plants are grid-connected, without storage systems and sun tracking systems.

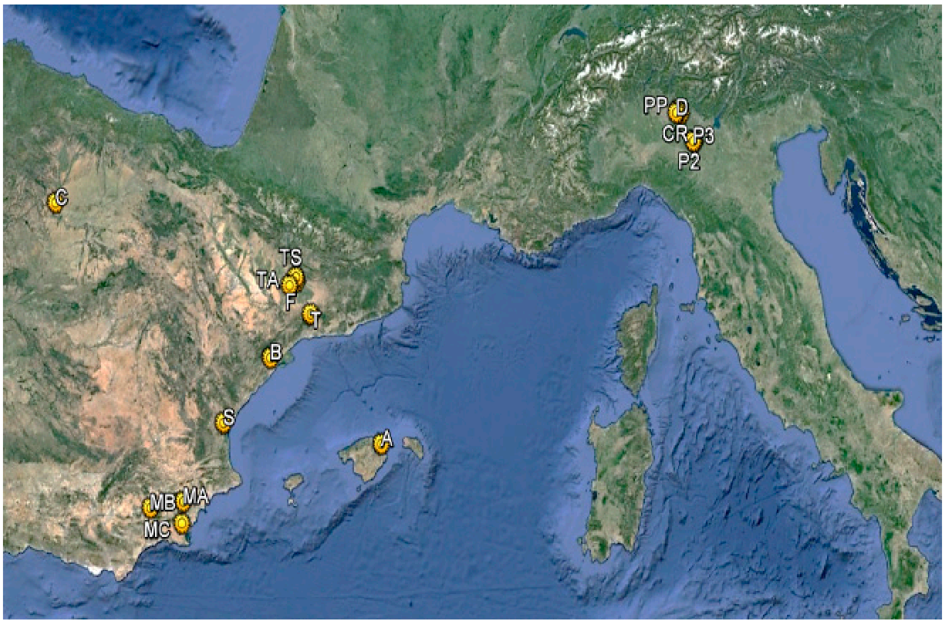

Figure 3. Geographical distribution of the PV plants.

Table 1 shows the location, typology, and configurations of the analysed plants.

The failures have been obtained from real data and provided by the responsible companies for the operation and maintenance of the PV systems. These failures have been mainly detected through the analysis of climatological and electrical data obtained from the monitoring system of the PV plant, the alarm system, the monitoring from the inverter, the field thermography measurements, and the visual inspection of the plants. All plants have had a daily professional supervision service. No failures were detected in alternating current wiring.

3.1. Failure Rates

Table 2 shows a breakdown of the total failures in each PV plant according to the previous parameters.

Table 2 shows the distribution of failure rates in each plant associated with the different elements.

As Table 3 shows, as the failure rates change significantly from one plant to another and from one element to another, it is difficult to assign an average value for failure rates.

The number of failures per year rate in a PV plant, *TFR*, changes between 3.2 and 93.60 failures/year, with a global average value of 25.49 failures/year. This rate is highly influenced by the size of the PV plant.

Per unit of installed equipment, the equipment with the highest failure rate is the monitoring system with an average failure rate of FRM = 10.4 failures/(year·monitoring system), (with a range between 1.6 and 37.6), followed by the inverter with an average failure rate of FRI_{in} = 0.701 failures/(year·inverter), the electrical grid with 0.53 failures/year, the transformer station with 0.494 failures/(year·transformer station), and the minor failure rate of the solar field, 0.00034081 failures/(year·module).

Table 1. Main characteristics of PV plants analysed. (Spain and Italy).

PV Parks Characteristics											
Location			**Type**	**Solar Field**			**Inverter**		**ST**	**Plant**	
PV Park	**PV Plant**	**Province**	**Ground/Roof**	**N° PV Modules**	**Material**	**Peak Power (Wp)**	**N° Inverters**	**Nominal Power (kW)**	**N° STs**	**Peak Power (kWp)**	**Nominal Power (kW)**
A	A-1	Mallorca	Ground	44,928	CdTe	75/77.5	2 4	500 540	3	3,425.8	3160
B	B-1 B-2	Castellón	Roof Roof	3465 2590	Si MC Si MC	238 305	7 7	100 100	1 1	824.7 789.9	700 700
C	C1	Zamora	Ground	57,888	CdTe	75	4	1000	4	4,341.6	4000
D	D-1	Cremona	Ground	16,200	CdTe	77.5	2	630	1	1,255.5	1260
F	F-1	Lérida	Roof	3754	Si PC	235	8	100	1	880.1	800
MA	MA-1	Murcia	Ground	25,812	CdTe	80	4	500	3	2,065.0	2000
MB	MB-1	Murcia	Ground	9540	Si PC	235	4	500	4	2,241.9	2000
MC	MC-1	Murcia	Ground	13,680	Si PC	230	6	500	3	3,146.4	3000
PP	PP-1	Palazzo P.	Ground	46,200	CdTe	77.5	2 3	800 630	3	3,580.5	3490
P2	P2-1	Parmense	Ground	20,520	CdTe	77.5	2	800	1	1,590.3	1600
P3	P3-1	Parmense	Ground	16,680	CdTe	77.5	2	630	1	1,292.7	1260
S	S-1 S-2	Valencia	Roof Roof	3266 3266	Si PC Si PC	230 230	1 1	630 630	1 1	751.2 751.2	630 630
T	T-1	Tarragona	Roof	5374	Si PC	215-235	10	100	1	1,218.6	1000
TA	TA-1 TA-2 TA-3	Lérida	Roof Roof Roof	520 520 5139	Si PC Si PC CdTe	220 220/225 77.5	20 14 4	5 5 100	1 1 1	114.4 81.3 398.0	100 70 400
TS	TS-1 TS-2	Lérida	Roof Roof	1587 1560	Si PC Si PC	215-235 235	22 24	15 15	1 1	354.6 366.1	330 360
Total											
15	20	-	Ground 9 Roof 6	282,489	Si PC 17.4% CdTe 82.6%	29.627 (MWp)	153	MAX 1000 MIN 5	34	29.470 (MWp)	27.490 (MW)

Table 2. Failures of the PV plants.

PV Park	Failures															TF
	Solar Field				Inverter				ST			Electrical Grid			Monitoring System	
	Modules	DC Wiring	Junction Box	TF_{SF}	Operation	Start up and Stopping	Monitoring	TF_{I}	Operation	Weather	TF_{ST}	Operation	Weather	TF_{G}	TF_{MS}	
A	24	0	1	25	7	2	9	18	3	1	4	0	1	1	3	54
B	0	2	0	2	2	0	0	2	0	0	0	0	0	0	34	38
C	13	0	1	14	1	0	2	3	4	0	4	2	0	2	4	31
D	8	0	0	8	0	0	0	0	0	0	0	1	0	1	11	20
F	0	0	0	0	0	0	2	2	0	0	0	0	0	0	20	22
MA	0	0	0	0	0	1	0	1	0	0	0	1	0	1	2	4
MB	0	0	1	1	3	0	0	3	0	0	0	2	0	2	4	10
MC	0	0	1	1	0	2	0	2	0	0	0	0	0	0	2	5
PP	45	0	0	45	1	4	0	5	4	1	5	1	0	1	3	63
P2	12	0	1	13	1	0	2	3	2	1	3	1	1	2	5	28
P3	11	0	0	11	0	0	0	0	2	3	5	0	0	0	4	22
S	0	0	0	0	0	0	0	0	0	0	0	0	0	0	4	4
T	0	0	0	0	2	1	0	3	0	0	0	0	0	0	26	29
TA	0	0	0	0	3	17	2	22	0	0	0	0	0	0	24	46
TS	0	0	0	0	38	30	2	70	0	0	0	0	0	0	47	117
Total	113	2	5	120	58	57	19	134	15	6	21	8	2	10	193	478

Table 3. Failure rates of the PV plants.

Failure Rates							
PV Parks	**FRSF**	**FRI**	**FRST**	**FRG**	**FRM**	**TFR**	**TFRp**
A	0.0004452	2.4	1.067	0.8	2.4	43.2	0.01367
B	0.0002642	0.114	0	0	27.2	30.4	0.02171
C	0.0001935	0.6	0.8	1.6	3.2	24.8	0.0062
D	0.0003951	0	0	0.8	8.8	16	0.0127
F	0	0.2	0	0	16	17.6	0.022
MA	0	0.2	0	0.8	1.6	3.2	0.0016
MB	0.0000839	0.6	0	1.6	3.2	8	0.004
MC	0.0000585	0.267	0	0	1.6	4	0.00133
PP	0.0007792	0.8	1.333	0.8	2.4	51.2	0.01467
P2	0.0005068	1.2	2.4	1.6	4	22.4	0.014
P3	0.0005276	0	4	0	3.2	17.6	0.01397
S	0	0	0	0	3.2	3.2	0.00254
T	0	0.24	0	0	20.8	23.2	0.0232
TA	0	0.463	0	0	19.2	36.8	0.06456
TS	0	1.217	0	0	37.6	93.6	0.13565
Total	**0.00034081**	**0.701**	**0.494**	**0.53**	**10.4**	**25.49**	**0.01739**

There are PV plants such as the TS with a high number of failures, 117, which represents 0.136 failures per year and kW. This is a roof PV plant, with Si-PC module, with 46 inverters of 15 kW. On the other side, there are PV plants such as S with very few failures, four, which represents 0.00256 failures per year and kW. This is a roof PV plant with Si-PC module too, but with two inverters of 630 kW. This shows that the relative number of failures have a great dependence on the size and configuration of each PV plant.

3.2. Failures and Energy Losses

3.2.1. Failures and Energy Losses under Criterion 1

Figure 4 shows the distribution of the total failures, *TF*, and the energy losses associated, *FEL*, in which TF_{SF}, TF_I, TF_{ST}, TF_G, and TF_{MS} are the total failures in the solar field, inverter, transformer station, electrical grid, and monitoring system, respectively, for all PV plants.

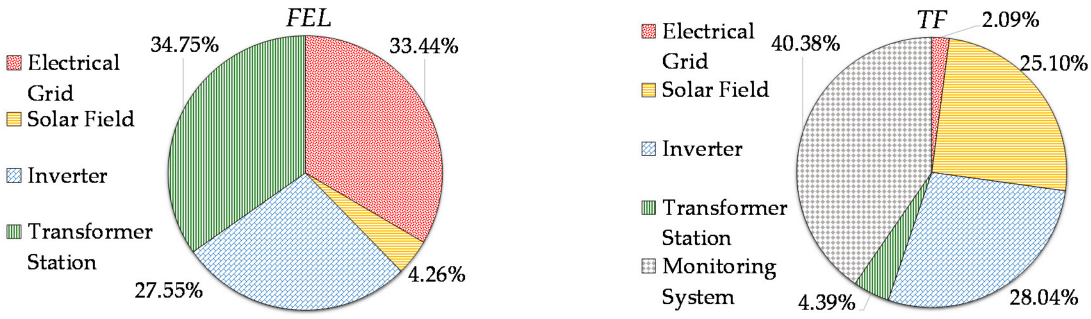

Figure 4. Distribution of *FEL* and *TF*.

We wish to highlight that the monitoring system is the responsible of most of the failures, but those failures do not have a significant impact on the energy production. It is necessary to emphasize that over 54% of failures in the monitoring system had a duration of less than 1 h. In addition, in most cases, failures were automatically repaired by their own monitoring system.

However, despite the minimum percentage, 6.48%, that the electrical grid and the transformer station failures represent, the energy losses associated with that equipment suppose, approximately, 68% of the total energy losses.

Figure 5 shows the distribution of the 120 failures in the solar field and their influence on the energy losses, *FEL*.

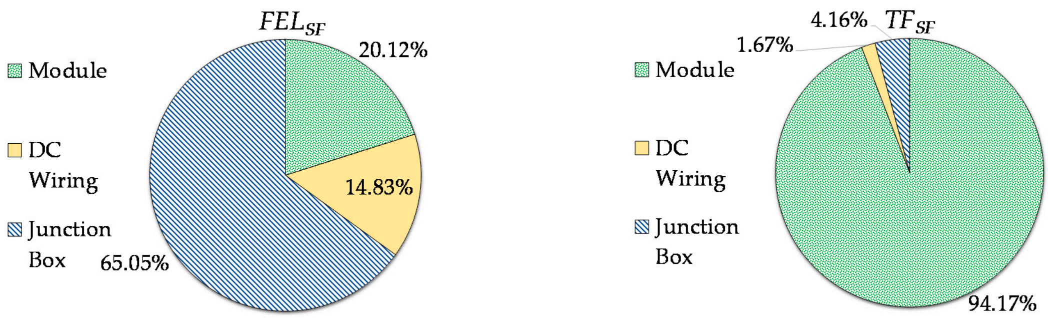

Figure 5. Distribution of failures and energy losses in the solar field.

Notice how most of the failures are caused due to the replacement of modules. This percentage would seem to be high a priori, but it should not be considered in that way taking into account that there are 282,489 PV modules between all the photovoltaic plants. Actually, the energy losses by replacing modules represent only the 20% of the energy losses in the solar field, as the influence of the non-production of one module is low compared to the influence on the energy losses of the wiring and junction boxes failures.

Figure 6 shows the distribution of the 134 failures of the inverters and their influence on the energy losses, *FEL*.

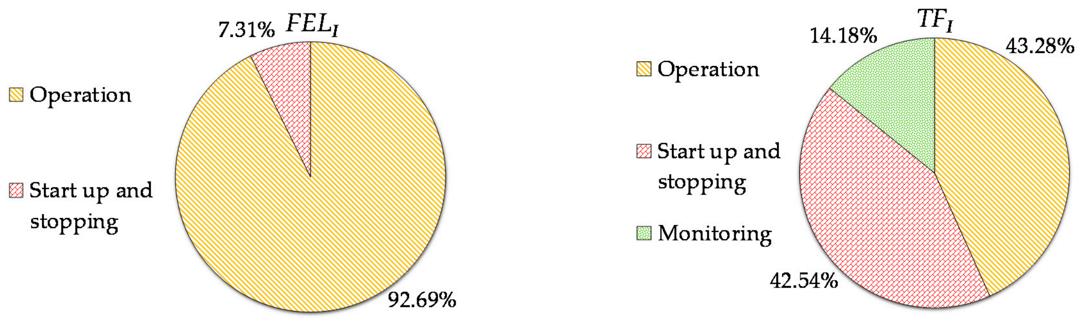

Figure 6. Distribution of failures and energy losses in the inverters.

According to Figure 6, approximately 14% of the failures are produced by the monitoring system that does not affect the energy production. Failures named operation failures of the inverter have a greater impact on production, as it is shown in this figure.

Table 4 shows a breakdown of failures of operation, start up, and stopping depending on the inverter power.

Table 4. Failures and energy losses according to the inverter power.

Power (kW)	Number of Inverters	Percentage of Failured Inverters	Operations Failures	Start-up and Stopping Failures	FEL_{IO} (kWh)	FEL_{StSp} (kWh)	FEL_I (kWh)	FEL_I/FEL
5	34	29.41%	1	12	3	2	5	0.01%
15	46	50.00%	38	30	1654	274	1928	1.21%
100	36	25.00%	5	8	2214	96	2310	1.45%
500	17	47.06%	7	4	12,243	2	12,244	7.68%
540	4	75.00%	4	2	20,249	1038	21,287	13.35%
630	8	12.50%	1	1	424	1664	2088	1.40%
800	4	25.00%	1	0	308	0	308	0.19%
1000	4	25.00%	1	0	3,595	0	3595	2.26%
Total	153	-	58	57	40,689	3077	43,766	27.55%

The results provided in Table 4 show that the inverters of power less or equal to 15 kW are the ones that have presented the highest number of failures, but their incidence in the energy losses do not exceed 1.5%.

Figure 5 shows the probability of an inverter having a number of failures $P_I(F)$.

Figure 7 shows that approximately 60% of the inverters have not presented any failure and that there are no inverters with more than 8 failures recorded in the analysed period.

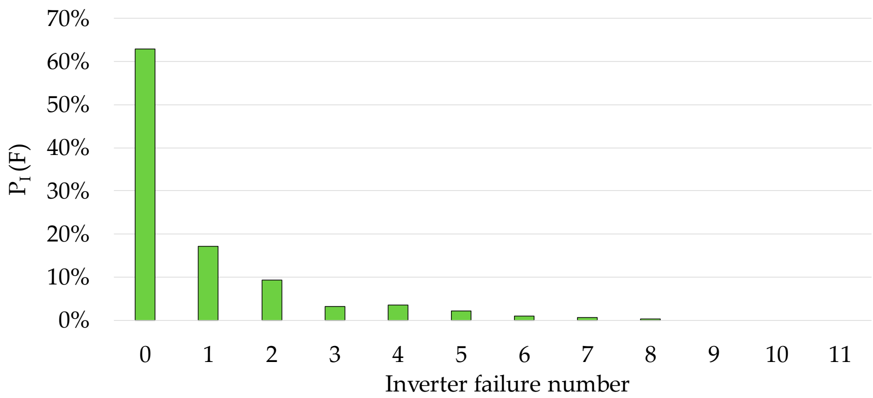

Figure 7. Probability of an inverter having a number of failures.

Figure 8 shows the distribution of the 23 failures of the transformer stations, TF_{ST}, and their influence on the energy losses, FEL_{ST}.

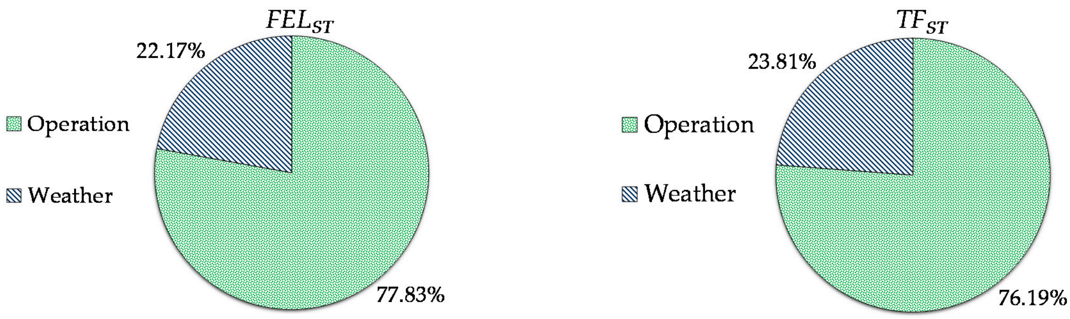

Figure 8. Distribution of failures and energy losses in the transformer station.

According to Figure 8, approximately 76% of the failures are caused by the action of the electrical protection setting. The relationship between the failures and the energy losses are practically the same.

Figure 9 shows the distribution of the 8 failures of the electrical grids, TF_{EG}.

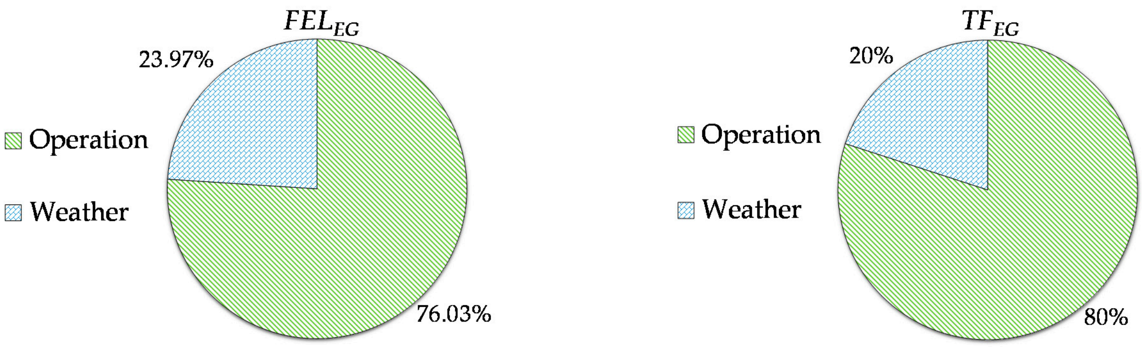

Figure 9. Distribution of failures and energy losses in the electrical grid.

According to Figure 9, over the 76% of the failures are caused due by electrical grid quality and exhibit, approximately, the same behaviour as the transformer station.

3.2.2. Failure and Energy Losses under Criterion 2

Figure 10 shows the distribution of failures and energy losses depending on the technology for all PV plants.

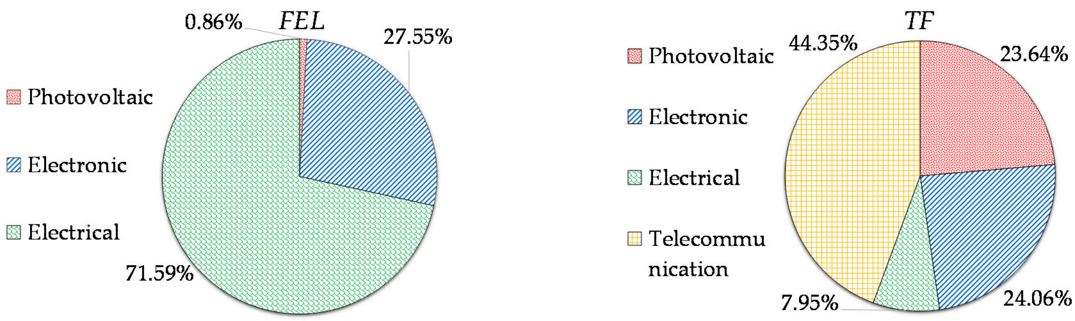

Figure 10. Distribution of failures and energy losses depending on technology.

Notice how TF_{TT} is the one presenting most failures, 42.05%, while TF_{PVT} represents 24.62% despite the large number of existing photovoltaic module units (282,489 modules). The percentage of failures associated with the photovoltaic technology only represents approximately 1% of energy losses, whereas the others technologies (excluding telecommunication) include the rest of energy losses with a slightly higher percentage.

3.3. Relative Impact of Failure and Inefficiencies on Energy Balance

Figure 11 shows the relative influence of *FEL* with respect to *RE* of each PV plant.

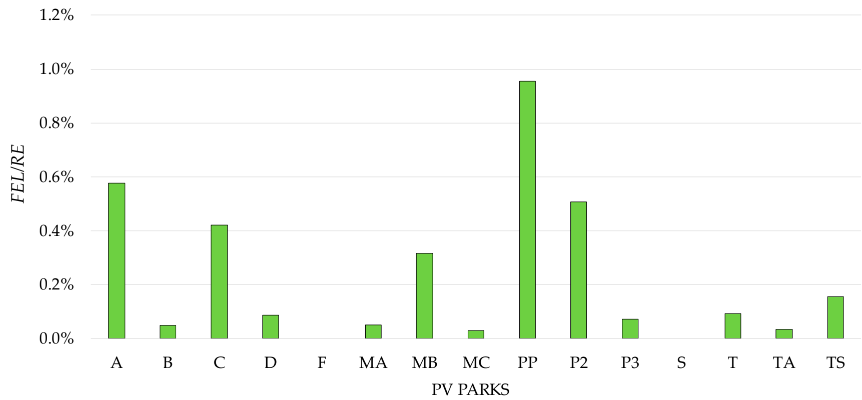

Figure 11. Relationship between *FEL* and *RE* in each PV plant.

FEL are not significant in all PV plants analysed and have not exceeded 1% of the energy produced. In addition, Figure 9 shows that this percentage varies from one photovoltaic plant to another, being null in the PV plants F and S, and being the maximum percentage, 0.96%, in the PP photovoltaic plant.

Figure 12 shows the percentage of *PEL* with respect to *RE* of each PV plant.

It is observed that *PEL* represent between 22.34% and 27.58% of the *RE* and are much higher than those associated with *FEL* that have been registered over the analysed period, as shown in Figure 11. Reducing *PEL* without modifying the design of the PV plants or changing the equipment is only possible by moving shadows and cleaning the solar field and improving the ventilation system of the inverter. Other failures that affect *PEL* such as mismatching losses, wiring losses, inverter, and transformer efficiency are difficult to improve.

Figure 13 shows a criticality matrix of the PV plant by combining the frequency of failures with energy losses in each element of the PV plant.

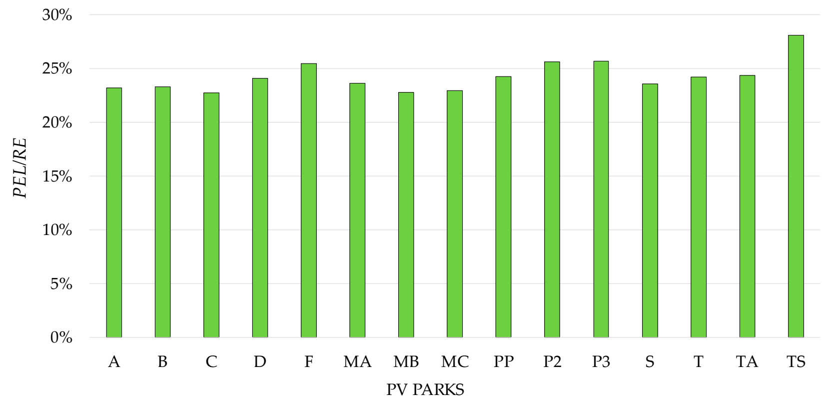

Figure 12. Relationship between the *PEL* and *RE* produced in each PV plant.

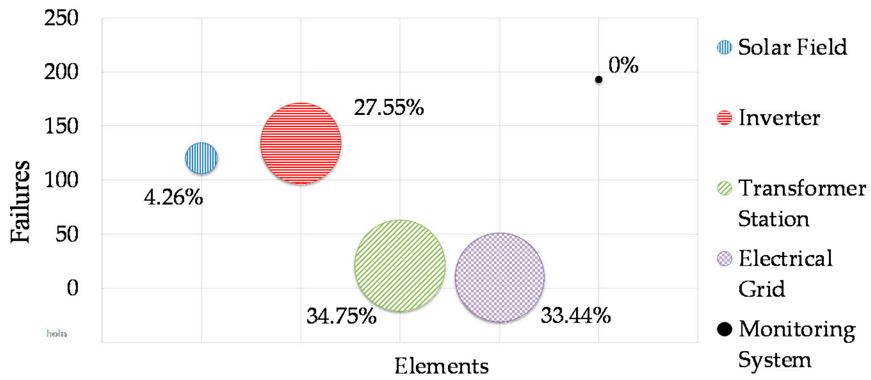

Figure 13. Quantitative comparison between number of failures and the percentage of the energy losses of each element of the PV plant (proportional to the size of the circle).

From the point of view of energy losses, according to Figure 13, the most critical types of equipment are the transformer station and the electrical grid, because they represent 68% of the energy losses in only 31 failures, while 32% of the remaining *FEL* are associated with the solar fields and inverters that had registered 254 failures. Energy losses associated with the solar field are very low. To complement the analysis, Figure 14 illustrates the ratio *FEL*/*TF* depending on the failure.

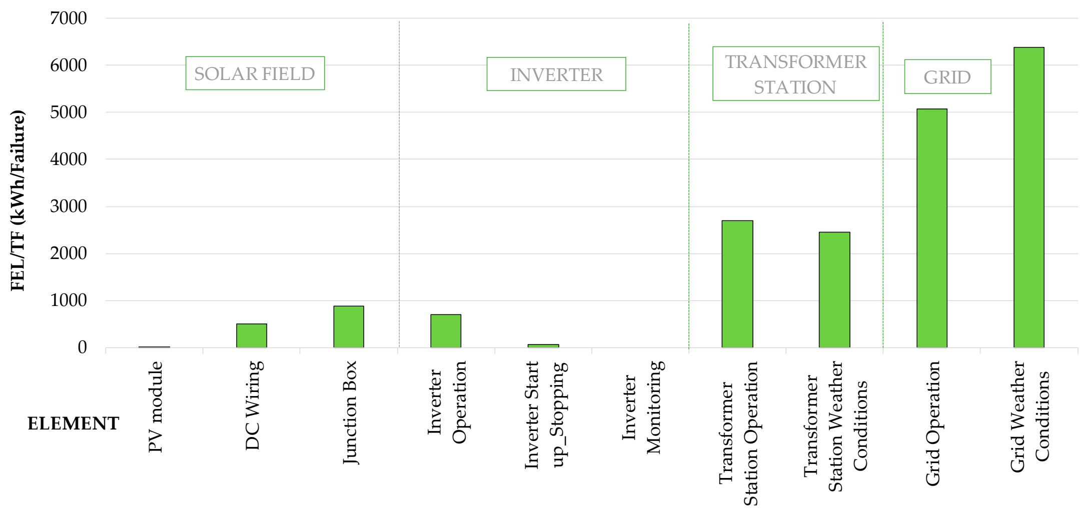

Figure 14. Relationship *FEL*/*TF* according to criterion 1 for all analysed PV plants.

Figure 14 shows effectively that the average energy losses associated with every failure are higher in the case of the electrical grid or transformer station than in inverters or solar field.

Figure 15 shows the mean time to repair (MTR), calculated as the average time from the instant of detection of the failure, t_d, and the instant of repair, t_r, depending on the failure, for all analysed PV plants.

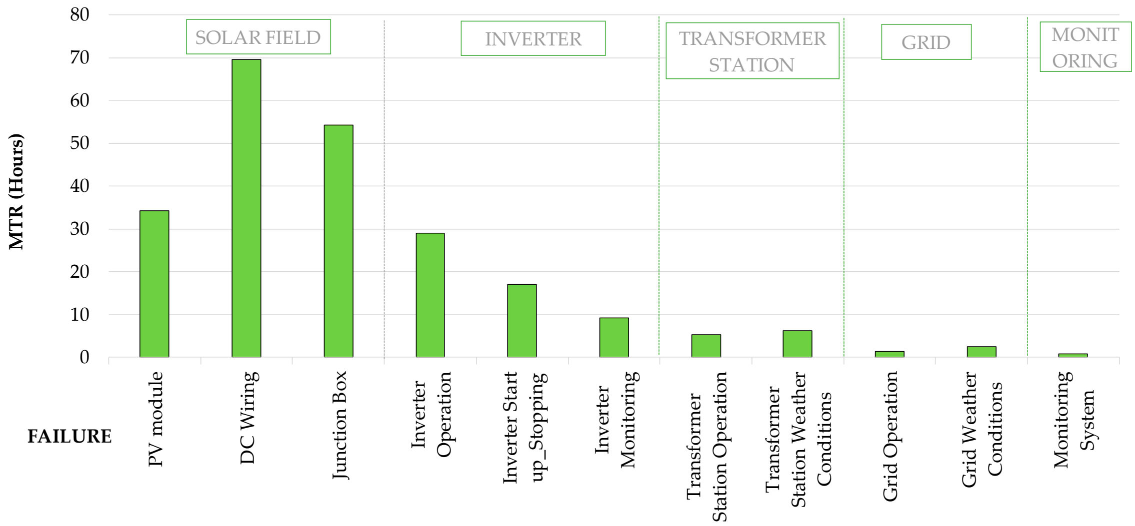

Figure 15. Mean time to repair according to criterion 1 for all analysed PV plants.

The average time to repair is indicative of the efficiency of the corrective maintenance tasks. In PV systems, time to repair has a non-uniform influence on the energy losses. There would be, necessarily, an analysis of the value of global solar radiation during the time to repair. This value is very linked to the season of the year and especially the hour of the day. In latitudes like Spain and North of Italy, a great difference exists between the diurnal hours and the solar radiation on the module plane depending on the season. Its means that failures in winter would have minor repercussion on energy losses that the same failures in summer time. So, to evaluate energy losses, more important than time to repair is the global solar radiation on the module plane during time to repair as it has been included in Appendix A equations.

Figure 15 shows that monitoring system has the lowest mean time to repair. This is because in many cases the monitoring system failure can be solved automatically or very quickly. Mean time to repair of the electrical grid has also been low due to the fact that electric utilities have experience in its supervision and tele-operation.

Although the major average time to repair has taken place in the solar field, solar field has the lowest energy losses, after monitoring system. It is due to the lower power that it is affected by a failure in the solar field.

4. Conclusions

This paper has shown the failures and energy balance of several real PV plants for 15 months, according to the indicated hypothesis. It has been observed that *PEL* have represented between 22.34% and 27.58% of *RE*. The influence of *FEL* on *RE* has been low in all analysed PV plants, with values between 0% and 0.96%. The influence of *FEL* on the energy balance of the PV plant has been much lower than *PEL*.

To avoid PV plant energy losses, the focus should be on *PEL* instead of *FEL*. Preventive maintenance to avoid *FEL* should be focused on inverters, the station transformer, and the electrical grid plant.

Solar field energy losses only represent 4.26% of all *FEL*. So, in accordance with the Anastasio study [33], high-resolution monitoring on the DC side does not seem to be critical, as most of the lost energy can be attributed to outages in the other subsystems such as the inverter and the AC subsystem. An alternative to high-resolution monitoring in the solar field may be to carry out thorough, preventive maintenance in the PV modules to detect the different kinds of failures in each period (perhaps five years or according to the warranty conditions over time).

Analysed PV plants are quite reliable, with an annual average number of failures of 25.49 failures/year. According to Table 3, failure rates have a great dependence on the characteristic of each PV plant (size and configuration).

Form the point of view of technology analysis, photovoltaic technology has been the most reliable technology of all.

Author Contributions: Isidoro Lillo-Bravo and Pablo González-Martínez conceived and designed the study; Jose Guasumba-Codena provided de information. All authors contributed analyzing the data; Miguel Larrañeta provided analysis tools; Pablo González-Martínez wrote the initial version of the paper that was lately revised by Isidoro Lillo-Bravo and Miguel Larrañeta.

Conflicts of Interest: The authors declare no conflict of interest.

Abbrevations

CdTe	Cadmium Telluride
FRG	Annual failure rate in the electrical grid of the PV plant
FRI	Annual failure rate in the inverter of the PV plant per inverter
FRM	Annual failure rate in the monitoring system of the PV plant
$FRSF$	Annual failure rate in the solar field of the PV plant per module
$FRST$	Annual failure rate in the transformer stations of the PV plant
FEL	Energy losses due to failures
FEL_{JB}	Total energy losses of all junction boxes of the PV plant
FEL_I	Total energy losses due to failures in the inverters of the PV plant
FEL_G	Total energy losses due to failures in the electrical grid of the PV plant
FEL_{SF}	Total energy losses due to failures in the solar fields of the PV plant
FEL_{ST}	Total energy losses due to failures in the transformer stations of the PV plant
GTI_t	Global tilted irradiance in the hour t on the module plane
ME	Maximum electrical output of a photovoltaic array
O&M	operation and maintenance
OPEX	operation and maintenance costs
PEL	Energy losses due to inefficiencies
$P_I\ (F)$	Probability of an inverter has a number of failures
P_n	Peak power of the PV plant in Standard Test Conditions
PR_{corr}	Hourly correct performance ratio
RE	Electrical energy yield at the feed-in meter
Si MC	Mono-crystalline silicon
Si PC	Poly-crystalline silicon
x-Si	Crystalline silicon
t_d	Hour in which the failure has been detected
t_r	Hour in which the failure has been repaired
TF	Total failures in the PV plant for 15 months
TF_G	Total failures in the electrical grid for 15 months
TFI	Total failures in the inverters for 15 months
TF_{MS}	Total failures in the monitoring system for 15 months
TF_{SF}	Total failures in the solar field for 15 months
TF_{ST}	Total failures in the transformer station for 15 months
TFR	Annual total failures rate of the PV plant
ΔT_{cell_t} (K)	The difference between the average hourly temperature of the PV reference module of the PV plant at hour t and 29,815 K

Appendix A

Equations used to calculate energy losses are the following:

The energy losses $FEL_{m(k,i,s)}$, associated with the failure and restitution of a module s of string i, of array k, from time t_d to time t_r, have been determined according to Equation (A1).

$$FEL_{m(k,i,s)} = Pn_{kis} \cdot S_k \cdot PR_{corr} \cdot \sum_{t=td}^{t=tr} \frac{GTI_t}{1000} \quad \text{(A1)}$$

in which Pn_{kis} is the power at STC of the PV module s of the string i, array k; and S_k is the number of module of the string i an PR_{corr} that is calculated for the 15 months period (h = 131,400 h) according to Equation (5).

The total energy losses associated with all the modules that have failed in the PV plant, FEL_m, have been determined according to Equation (A2).

$$FEL_m = \sum_{k=1}^{k} FEL_{m(k,i,s)} \quad \text{(A2)}$$

Energy losses due to wiring failures within a string i, $FEL_{SS(k,i,s)}$, which have failed from time t_d to time t_r, in the array k, have been determined according to Equation (A3).

$$FEL_{SS(k,i,s)} = Pn_{kis} \cdot S_k \cdot PR_{corr} \cdot \sum_{t=td}^{t=tr} \frac{GTI_t}{1000} \quad \text{(A3)}$$

The total energy losses due to wiring failures of the PV plant, FEL_{SSS}, have been determined according to Equation (A4).

$$FEL_{SSS} = \sum_{k=1}^{k} FEL_{SS(k,i,s)} \quad \text{(A4)}$$

Energy losses of a wiring failure that leaves the junction box b, with i_b strings connected, in the array k, $FEL_{SS(k,b)}$, from time t_d to time t_r, have been determined according to Equation (A5).

$$FEL_{SS(k,b)} = Pn_{kis} \cdot S_k \cdot i_b \cdot PR_{corr} \cdot \sum_{t=td}^{t=tr} \frac{GTI_t}{1000} \quad \text{(A5)}$$

in which i_b is the number of strings connected to the junction box b.

The total energy losses due to wiring failure of the PV plant, FEL_{SSB}, have been determined according to Equation (A6).

$$FEL_{SSB} = \sum_{k=1}^{k} \sum_{b=1}^{b} FEL_{SS(k,b)} \quad \text{(A6)}$$

in which b is the number of junction boxes in the plant array k.

The total energy losses in failures in DC wiring, FEL_{SST}, have been determined according to Equation (A7).

$$FEL_{SST} = FEL_{SSS} + FEL_{SSB} \quad \text{(A7)}$$

Energy losses due to failures in the junction box in the array k, $FEL_{JB(k,b,i_k)}$, which has failed from time t_d to time t_r and causes the loss of the energy of i_k strings connected to it, have been determined according to Equation (A8).

$$FEL_{JB(k,b,i_k)} = Pn_{kis} \cdot S_k \cdot i \cdot PR_{corr} \cdot \sum_{t=td}^{t=tr} \frac{GTI_t}{1000} \quad \text{(A8)}$$

The total energy losses of all junction boxes of the PV plant, FEL_{JB}, have been determined according to Equation (A9).

$$FEL_{JB} = \sum_{k=1}^{k} \sum_{b=1}^{b} FEL_{JB(k,b,i_k)} \tag{A9}$$

The total energy losses in all solar fields of the PV plant, FEL_{SF}, have been determined according to Equation (A10).

$$FEL_{SF} = FEL_m + FEL_{JB} + FEL_{SST} \tag{A10}$$

Energy losses due to an inverter operation failure connected, FEL_{IOK}, from time t_d to time t_r, have been determined according to Equation (A11).

$$FEL_{IOK} = Pn_k \cdot PR_{corr} \cdot \sum_{t=td}^{t=tr} \frac{GTI_t}{1000} \tag{A11}$$

in which Pn_k is the sum of the peak power of the modules in STC connected to the inverter.

The total energy losses due to operation failures of all inverters of the PV plant, FEL_{IO}, have been determined according to Equation (A12).

$$FEL_{IO} = \sum_{k=1}^{k} FEL_{IOk} \tag{A12}$$

Energy losses due to start up and stopping failure of inverter k in the PV plant, FEL_{StSpk}, from the time t_d to time t_r, have been determined according to Equation (A13).

$$FEL_{StSpk} = Pn_k \cdot PR_{corr} \cdot \sum_{t=td}^{t=tr} \frac{GTI_t}{1000} \tag{A13}$$

The total energy losses due to start up and stopping failures of all inverters of the PV plant, FEL_{StSp}, have been determined according to Equation (A14).

$$FEL_{StSp} = \sum_{k=1}^{k} FEL_{StSpk} \tag{A14}$$

The total energy losses due to failures of inverters of the PV plant, FEL_I, have been determined according to Equation (A15).

$$FEL_I = FEL_{IO} + FEL_{StSp} \tag{A15}$$

Energy losses due to operation failures of the transformer station of the PV plant, FEL_{STOa}, from the time t_d to time t_r, have been determined according to Equation (A16).

$$FEL_{STOa} = P_{pSTa} \cdot PR_{corr} \cdot \sum_{t=td}^{t=tr} \frac{GTI_t}{1000} \tag{A16}$$

P_{pSTa} is the sum of the peak power in STC of all modules connected to the transformer station of the PV plant.

The total energy losses due to total operation failures in all transformer station of the PV plant, FEL_{STO}, have been determined according to Equation (A17).

$$FEL_{STO} = \sum_{a=1}^{a} FEL_{STOa} \tag{A17}$$

Energy losses due to weather failures of the transformer station a, FEL_{STWa}, from time t_d to time t_r, have been determined according to Equation (A18).

$$FEL_{STWa} = P_{pSTa} \cdot PR_{corr} \cdot \sum_{t=td}^{t=tr} \frac{GTI_t}{1000} \tag{A18}$$

The total energy losses due to total weather failures in all transformer station of the PV plant, FEL_{STW}, have been determined according to Equation (A19).

$$FEL_{STW} = \sum_{a=1}^{a} FEL_{STWa} \tag{A19}$$

in which a is the number of transformer stations of the PV plant.

The total energy losses due to failures in the transformer stations of the PV plant, FEL_{ST}, have been determined according to Equation (A20).

$$FEL_{ST} = FEL_{STO} + FEL_{STW} \tag{A20}$$

Energy losses due to operation failures of the electrical grid, FEL_{GO}, from time t_d to time t_r, have been determined according to Equation (A21).

$$FEL_{GO} = P_n \cdot PR_{corr} \cdot \sum_{t=td}^{t=tr} \frac{GTI_t}{1000} \tag{A21}$$

Energy losses due to weather failures of the electrical grid, FEL_{GW}, from time t_d to time t_r, have been determined according to Equation (A22).

$$FEL_{GW} = P_n \cdot PR_{corr} \cdot \sum_{t=td}^{t=tr} \frac{GTI_t}{1000} \tag{A22}$$

The total energy losses due to failures in the electrical grid of the PV plant, FEL_n, have been determined according to Equation (A23).

$$FEL_G = FEL_{GW} + FEL_{GO} \tag{A23}$$

The total energy losses due to failures, FEL, in the PV plant, have been determined according to Equation (A24).

$$FEL = FEL_{SF} + FEL_I + FEL_{ST} + FEL_G \tag{A24}$$

When referring to the set of PV plants, they add up to all n plants. Thus, all energy losses by failures of all plants would result according to Equation (A25).

$$FEL = \sum_{n=1}^{n} FEL_n \tag{A25}$$

References

1. International Renewable Energy Agency. *The Power to Change: Solar and Wind Cost Reduction Potential to 2025*; International Renewable Energy Agency (IRENA): Abu Dhabi, United Arab Emirates, 2016; ISBN 978-92-95111-97-4.
2. David, M.; Jahn, U.; Tjengdrawira, C.; Theologitis, I.T. "Technical risks in PV projects—Report on technical risks in PV project development and PV plant operation" Solar Bankability. Available online: http://www.solarbankability.org/fileadmin/sites/www/files/documents/D1.1_2.1_Technical_risks_in_PV_projects.pdf (accessed on 2 January 2018).

3. Kim, N.; Hwang, K.; Kim, D.; Lee, J.H.; Jeong, D.H. Analysis and reproduction of snail trails on silver grid lines in crystalline silicon photovoltaic modules. *Sol. Energy* **2016**, *124*, 153–162. [CrossRef]
4. Köntges, M.; Kurtz, S.; Jahn, U.; Berger, K.A.; Kato, K.; Friesen, T.; Liu, H.; van Iseghem, M. *Review of Failures of Photovoltaic Modules 2014*; Report IEA-PVPS T13-01:2014; Institute for Solar Energy Research Hamelin: Emmerthal, Germany, 2014; ISBN 978-3-906042-16-9.
5. Sporleder, K.; Hübener, K.; Petter, K.; Kranert, C.; Luka, T.; Tureka, M. Light induced degradation: Kinetic model and grain boundary impact on sponge-LID. *Energy Procedia* **2017**, *124*, 174–179. [CrossRef]
6. Mavromatakis, F.; Vigmola, F.; Marion, B. Low irradiance losses of photovoltaic modules. *Sol. Energy* **2017**, *157*, 496–506. [CrossRef]
7. Kaden, T.; Lammers, K.; Möller, H.J. Power loss prognosis from thermographic images of PID affected silicon solar modules. *Sol. Energy Mater. Sol. Cells* **2015**, *142*, 24–28. [CrossRef]
8. Pareek, S.; Chaturvedi, N.; Dahiya, R. Optimal interconnections to address partial shading losses in solar photovoltaic arrays. *Sol. Energy* **2017**, *155*, 537–551. [CrossRef]
9. Marion, B.; Schaefer, R.; Caine, H.; Sanchez, G. Measured and modeled photovoltaic system energy losses from snow for Colorado and Wisconsin location. *Sol. Energy* **2013**, *97*, 112–121. [CrossRef]
10. Racharla, S.; Rajan, K. Solar tracking system—A review. *Int. J. Sustain. Eng.* **2017**, *10*, 27–81.
11. Potnuru, S.R.; Pattabiraman, D.; Ganesan, S.I.; Chilakapati, N. Positioning of PV panels for reduction in line losses and mismatch losses in PV array. *Renew. Energy* **2017**, *78*, 264–275. [CrossRef]
12. Lappalainen, K.; Valkealahti, S. Photovoltaic mismatch losses caused by moving clouds. *Sol. Energy* **2017**, *158*, 455–461. [CrossRef]
13. Alam, M.; Khan, F.; Johnson, J.; Flicker, J. A comprehensive review of catastrophic faults in PV arrays: Types, detection, and mitigation techniques. *IEEE J. Photovolt.* **2015**, *5*, 1–16. [CrossRef]
14. Hasselbrink, M.; Anderson, Z.; Defreitas, M.; Mikofski, Y.-C.; Shen, S.; Caldwell, A.; Terao, D.; Kavulak, Z.; Campeau, Z.; DeGraaff, D. Site Data Validation of the PVLife model using 3 Million Module-Years of Live. In Proceedings of the 39th IEEE PVSC Tampa, Tampa, FL, USA, 16–21 June 2013; pp. 7–12.
15. Jordan, D.C.; Silverman, T.J.; Wohlgemuth, J.H.; Kurtz, S.R.; van Sant, K.T. Photovoltaic Failure and Degradation Modes. *Prog. Photovolt.* **2017**, *25*, 318–326. [CrossRef]
16. Jordan, D.C.; Kurtz, S.R. Photovoltaic Degradation Rates—An Analytical Review. *Prog. Photovolt. Res. Appl.* **2013**, *21*, 12–29. [CrossRef]
17. Wei, L.; Kerkman, R.J.; Lukaszewski, R.A.; Brown, B.P.; Gollhardt, N.; Weiss, B.W. Junction temperature prediction of a multiple-chip IGBT module under DC condition. In Proceedings of the 41st IAS Annual Meeting Conference Record of the IEEE Industry Applications Conference, Tampa, FL, USA, 8–12 October 2006; pp. 754–762.
18. Saravanan, S.; Babu, N.R. Maximum power point tracking algorithms for photovoltaic system—A review. *Renew. Sustain. Energy Rev.* **2017**, *57*, 192–204. [CrossRef]
19. Harb, S.; Balog, R.S. Reliability of candidate photovoltaic module-integrated inverter topologies. In Proceedings of the Twenty-Seventh Annual IEEE Applied Power Electronics Conference and Exposition. (APEC), Orlando, FL, USA, 5–9 February 2012; pp. 898–903.
20. Flicker, J.; Kaplar, R.; Marinella, M.; Granata, J. PV inverter performance and reliability: What is the role of the bus capacitor? In Proceedings of the IEEE 38th Photovoltaic Specialists Conference (PVSC), Austin, TX, USA, 3–8 June 2012; Volume 2, pp. 1–3.
21. Chan, F.; Calleja, H.; Martinez, E. Grid connected PV systems: A reliability based comparison. In Proceedings of the IEEE International Symposium on Industrial Electronics, Montreal, QC, Canada, 9–13 July 2006; pp. 1–6.
22. Zhang, P.; Li, W.; Li, S.; Wang, Y.; Xiao, W. Reliability assessment of photovoltaic power systems: Review of current status and future perspectives. *Appl. Energy* **2013**, *104*, 822–833. [CrossRef]
23. Seguin, R.; Woyak, J.; Costyk, D.; Hambrick, J. *High-Penetration PV Integration Handbook for Distribution Engineers*; Technical Report NREL/TP-5D00-63114; National Renewable Energy Laboratory: Denver W Pkwy, CO, USA, 2016.
24. Nikolovski, S.; Papuga, V.; Knežević, G.; Fekete, K. Relay protection coordination for photovoltaic power plant connected on distribution network. Case study. *Int. J. Electr. Comput. Eng. Syst.* **2014**, *5*, 15–20.

25. Dhople, S.V.; Davoudi, A.; Chapman, P.L.; Domínguez-García, A.D. Integrating photovoltaic inverter reliability into energy yield estimation with markov models. In Proceedings of the 12th Workshop on Control and Modeling for Power Electronics (COMPEL), Boulder, CO, USA, 28–30 June 2010; pp. 1–5.
26. Sarr, O.N.; Barro, F.I.; Niasse, O.A.; Dia, F.; Mbengue, N.; Ba, B.; Sene, C. Analysis of Failure Modes Effect and Criticality Analysis (FMECA): A stand-alone photovoltaic system. *Sci. J. Energy Eng.* **2017**, *5*, 40–47. [CrossRef]
27. Wang, H.; Zhu, N.; Bai, X. Reliability model assessment of grid-connected solar photovoltaic system based on Monte-Carlo. *Appl. Sol. Energy* **2015**, *51*, 262–266. [CrossRef]
28. Gupta, N.; Garg, R. Parmod Kumar Sensitivity and reliability models of a PV system connected to grid. *Renew. Sustain. Energy Rev.* **2017**, *69*, 188–196. [CrossRef]
29. Mustafa, A.M.; Omran, W.A.; Hegazy, Y.G.; Abu-Elnaga, M.M. Reliability assessment of grid connected photovoltaic generation systems. In Proceedings of the International Conference on Renewable Energy Research and Applications (ICRERA), Palermo, Italy, 22–25 November 2015; pp. 22–25.
30. Van Sark, W.; Reich, N.H.; Müller, B.; Reise, C. Review of PV performance ratio development. In Proceedings of the 28th World Renewable Energy Forum, WREF 2012, Including World Renewable Energy Congress XII and Colorado Renewable Energy Society (CRES) Annual Conference, Denver, CO, USA, 13–17 May 2012.
31. Zhang, L.; Zhou, Y.; Flynn, D.; Mutale, J.; Mancarella, P. System-level operational and adequacy impact assessment of photovoltaic and distributed energy storage, with consideration of inertial constraints, dynamic reserve and interconnection flexibility. *Energies* **2017**, *10*, 989. [CrossRef]
32. Grunow, P.; Lust, S.; Sauter, D.; Hoffmann, V.; Beneking, C.; Litzenburger, B.; Podlowski, L. Weak light performance and annual yields of PV modules and systems as a result of the basic parameter set of industrial solar cells. In Proceedings of the 19th European Photovoltaic Solar Energy Conference, Paris, France, 7–11 June 2004.
33. Mishra, N.; Yadav, A.S.; Pachauri, R.; Chauhan, Y.K.; Yadav, V.K. Performance enhancement of PV system using proposed array topologies under various shadow patterns. *Sol. Energy* **2017**, *157*, 641–656. [CrossRef]
34. Pierro, M.; Bucci, F.; Cornaro, C. Impact of light soaking and thermal annealing on amorphous silicon thin film performance. *Prog. Photovolt. Res. Appl.* **2015**, *23*, 1581–1596. [CrossRef]
35. Cornaro, C.; Pierro, M.; Moser, D.; Garrido, G.N.; Alonso-Abella, M.; Gueymard, C.A. Outdoor Characterization of CdTe Technology and Seasonal Performance Analysis at Different Latitudes in Europe. In Proceedings of the 33rd European Photovoltaic Solar Energy Conference and Exhibition, Amsterdam, The Netherlands, 25–29 September 2017.
36. Pierro, M.; Bucci, F.; Cornaro, C. Full characterization of photovoltaic modules in real operating conditions: Theoretical model, measurement method and results. *Prog. Photovolt. Res. Appl.* **2014**, *23*, 443–461. [CrossRef]
37. Zhang, Z.; Wang, L.; Kurtz, S.; Wu, J.; Zhu, Z.W. Operating temperatures of open-rack installed photovoltaic inverters. *Sol. Energy* **2016**, *137*, 344–351. [CrossRef]
38. Tobón, A.; Peláez-Restrepo, J.; Villegas-Ceballos, J.P.; Serna-Garcés, S.I.; Herrera, J.; Ibeas, A. Maximum power point tracking of photovoltaic panels by using improved pattern search methods. *Energies* **2017**, *10*, 1316. [CrossRef]
39. Zini, G.; Mangeant, C.; Merten, J. Reliability of large-scale grid-connected photovoltaic systems. *Renew. Energy* **2011**, *36*, 2334–2340. [CrossRef]
40. Golnas, A. PV System Reliability: An Operator's Perspective. In Proceedings of the IEEE 38th Photovoltaic Specialists Conference (PVSC) Part 2, Austin, TX, USA, 3–8 June 2012; pp. 2156–3381.
41. Jahn, U.; Herz, M. Managing Technical Risks in PV Investments: How to Quantify the Impact of Risk Mitigation Measures for Different PV Project Phases? Available online: https://doi.org/10.1002/pip.2970 (accessed on 2 January 2018).
42. Wittmer, B.; Mermoud, A.; Schott, T. Analysis of PV grid installations performance, comparing measured data to simulation results to identify problems in operation and monitoring. In Proceedings of the 30th European Photovoltaic Solar Energy Conference and Exhibition, Hamburg, Germany, 14–18 September 2015.
43. System Advisor Model Version 2016.3.14 (SAM 2016.3.14). National Renewable Energy Laboratory: Golden, CO, USA. Available online: https://sam.nrel.gov/content/downloads (accessed on 31 October 2016).
44. Kurtz, S.; Riley, E.; Newmiller, J.; Dierauf, T.; Kimber, A.; McKee, J.; Flottemesch, R.; Krishnani, P. *Analysis of Photovoltaic System Energy Performance Evaluation Method*; Technical Report NREL/TP-5200-60628; NREL: Golden, CO, USA, 2013. Available online: www.nrel.gov/publications (accessed on 2 January 2018).

45. International Electrotechnical Commission. *International Electrotechnical Vocabulary Chapter 191, Dependability and Quality of Service*; International Standard: IEC 60050-191; International Electrotechnical Commission: Geneva, Switzerland, 1990.
46. Dierauf, T.; Growitz, A.; Kurtz, S.; Cruz, J.L.B.; Riley, E.; Hansen, C. *Weather-Corrected Performance Ratio*; Technical Report NREL/TP-5200-57991; NREL: Golden, CO, USA, 2013. Available online: http://www.nrel.gov/docs/fy13osti/57991.pdf (accessed on 2 January 2018).